

PEGAsus: 3D Personalization of Geometry and Appearance

JINGYU HU, The Chinese University of Hong Kong, HK SAR, China

BIN HU, The University of Hong Kong, HK SAR, China

KA-HEI HUI, Autodesk Research, Canada

HAIPENG LI, The Hong Kong University of Science and Technology , HK SAR, China

ZHENGZHE LIU*, Lingnan University, HK SAR, China

DANIEL COHEN-OR, Tel-Aviv University, Israel

CHI-WING FU, The Chinese University of Hong Kong, HK SAR, China

We present PEGAsus, a new framework capable of generating Personalized 3D shapes by learning shape concepts at both Geometry and Appearance levels. First, we formulate 3D shape personalization as extracting reusable, category-agnostic geometric and appearance attributes from reference shapes, and composing these attributes with text to generate novel shapes. Second, we design a progressive optimization strategy to learn shape concepts at both the geometry and appearance levels, decoupling the shape concept learning process. Third, we extend our approach to region-wise concept learning, enabling flexible concept extraction, with context-aware and context-free losses. Extensive experimental results show that PEGAsus is able to effectively extract attributes from a wide range of reference shapes and then flexibly compose these concepts with text to synthesize new shapes. This enables fine-grained control over shape generation and supports the creation of diverse, personalized results, even in challenging cross-category scenarios. Both quantitative and qualitative experiments demonstrate that our approach outperforms existing state-of-the-art solutions.

1 Introduction

Creating distinctive 3D assets is a tedious and expensive process. Often, significant iterations are required to create a desired 3D design. So, after investing huge effort in making a design, artists typically seek to reuse a design’s geometric/appearance attributes to create some other designs, rather than creating new ones completely from scratch. Yet, such reusability is hard to achieve, especially for general 3D objects. To reuse geometric/appearance attributes requires not only the capability to identify and extract geometric/appearance attributes in the reference object but also the capability to incorporate the attributes to create new designs with controllability.

Existing methods struggle to achieve such a goal. Classical example-based 3D modeling methods [Bokeloh et al. 2010; Chaudhuri et al. 2011; Funkhouser et al. 2004] generally reuse a reference shape by assembling retrieved parts. This approach is essentially heuristic and operates at part level, offering limited semantic control in attribute extraction and incorporation. 3D stylization [Hu et al. 2017; Li et al. 2013; Xu et al. 2010] is another closely related approach, aiming to transfer the style of a reference shape to modify a given target shape. Yet, the approach assumes a given target shape. It *cannot* directly generate new shapes guided solely by the reference. This reliance limits its usability in 3D asset design, where artists

*Corresponding author.

Authors’ Contact Information: Jingyu Hu, The Chinese University of Hong Kong, HK SAR, China; Bin Hu, The University of Hong Kong, HK SAR, China; Ka-Hei Hui, Autodesk Research, Canada; Haipeng Li, The Hong Kong University of Science and Technology , HK SAR, China; Zhengzhe Liu, Lingnan University, HK SAR, China; Daniel Cohen-Or, Tel-Aviv University, Israel; Chi-Wing Fu, The Chinese University of Hong Kong, HK SAR, China.

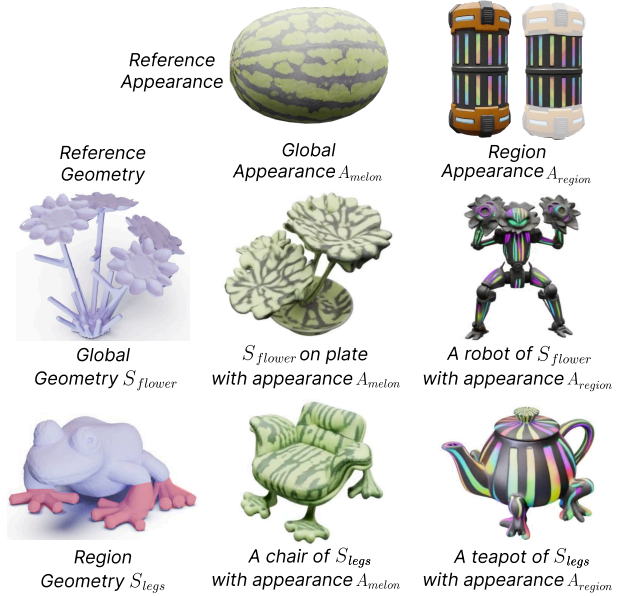


Fig. 1. PEGAsus is capable of extracting shape concepts for the global appearance of a watermelon, region-wise appearance of a stripe pattern, global geometry of a flower, and region-wise geometry of frog legs, then composing these learned concepts with text prompts in different ways to synthesize the four new shapes shown above, e.g., a chair whose lower part follows the frog legs and appearance follows the watermelon.

often want to create new designs, even across shapes of different categories, without requiring efforts to pre-model the target.

In this work, we pursue 3D personalization. We aim to learn attributes from references to guide the shape generation, without prescribing a target instance. While this paradigm has been explored in image generation [Gal et al. 2023; Kumari et al. 2023; Ruiz et al. 2023], extending it to 3D presents unique challenges. Unlike 2D images, where attributes are entangled, 3D asset design requires explicitly decoupling the attribute controls over geometry and appearance, while supporting region-wise concept learning and cross-category reusability; see Figure 1 for a preview of our results.

In this paper, we introduce PEGAsus, short for 3D **PE**ersonalization of **G**eometry and **A**ppearance (PEGAsus), reflecting its focus on learning reusable shape concepts applicable beyond a single instance or category. From a reference shape, PEGAsus can effectively learn reusable and category-agnostic shape concepts, where each concept

captures a specific geometric/appearance attribute. The learned concepts can then be composed with text to synthesize new shapes, while preserving the attributes extracted from the reference.

To achieve this, we build our framework on TRELLIS [Xiang et al. 2025], a large 3D foundation model, which naturally decouples geometry and appearance through a two-stage shape generation pipeline. Leveraging this model as a robust prior, we design a progressive optimization strategy to extract geometry- and appearance-level concepts from different stages of the pipeline, allowing their concepts to be learned independently. Further, PEGAsus supports both global concept learning from the entire shape and a region-wise mechanism that localizes the concept learning on a user-specified region. For region-wise concept learning, we introduce two complementary objectives: the context-aware loss to ensure visual coherence and the context-free loss to isolate the concept learning from the region’s surroundings. The learned concept is jointly represented by an optimized text embedding and a fine-tuned generator. At inference, the concept embedding can be composed with text and fed into the fine-tuned generator to synthesize new shapes.

PEGAsus supports four personalization modes: { global or region-wise concept learning } \times { geometry or appearance }. As Figure 1 shows, PEGAsus is able to extract the global geometry concept of the flower, the region geometry concept of the frog’s legs, global appearance concept of the watermelon, and region appearance concept of the striped pattern, and then flexibly reuse and compose these concepts with texts to synthesize different new shapes.

In summary, we make the following contributions:

- We formulate the problem of *3D shape personalization* as extracting reusable, category-agnostic geometric and appearance attributes from reference shapes and composing the attributes with text to generate new shapes.
- We propose a concept-level 3D generation framework that independently learns and composes geometry-level and appearance-level shape concepts, while flexibly supporting both global and region-wise personalization.
- Both quantitative and qualitative results show that PEGAsus is able to produce a wide range of novel personalized 3D shapes with four distinct personalization modes, outperforming existing methods in both quality and flexibility.

2 Related Work

Prior related work spans several directions, exploring different ways of generating, editing, or adapting 3D content, from part-based synthesis and style propagation to large-scale generative modeling and concept learning. Below, we briefly review these areas and position our approach with respect to their assumptions and limitations.

Example-based 3D Modeling [Funkhouser et al. 2004] aims to synthesize new shapes by copying, deforming, and assembling parts from a database of exemplar shapes. Subsequent works [Bokeloh et al. 2010; Chaudhuri et al. 2011; Fisher et al. 2012; Kalogerakis et al. 2012; Merrell 2007; Merrell and Manocha 2008; Xu et al. 2012; Zhou et al. 2007] extend this paradigm with probabilistic modeling or part-based composition. Their reliance on manual decomposition or handcrafted priors, e.g., symmetry, however, restricts the synthesis

to a recombination of database components, limiting the generalization to novel or cross-category scenarios. Recently, learning-based methods [Li et al. 2023; Maruani et al. 2025; Wu et al. 2024b; Wu and Zheng 2022] adopt generative models to implicitly extract regions or patches for producing plausible shape variants from a single reference shape. These approaches, however, focus primarily on exemplar-specific diversity, e.g., modify the aspect ratio of the exemplar shape, offering limited semantic control over the generated shapes. In contrast, our method learns reusable, category-agnostic attributes from the reference shape, enabling more flexible semantic control. The extracted attributes can be composed with texts to synthesize new shapes, even for cross-category scenarios.

3D stylization. Given a reference style input and a target content shape, 3D stylization aims to extract the stylistic patterns of the reference and re-apply them to the target to synthesize new shapes. This approach operates across various representations, including explicit meshes [Hertz et al. 2020; Höllerin et al. 2022; Hu et al. 2017; Kato et al. 2018; Li et al. 2013; Michel et al. 2022; Xu et al. 2010; Yin et al. 2021], neural implicit fields, and Gaussian splatting [Fan et al. 2022; Huang et al. 2021, 2022; Kumar et al. 2023; Liu et al. 2023b; Nguyen-Phuoc et al. 2022; Zhang et al. 2025, 2023a]. To enhance the generalizability, recent approaches [Chen et al. 2025; Dong et al. 2024; Xie et al. 2024] leverage strong 2D priors from large-scale image diffusion models [Rombach et al. 2022] for 3D stylization. Meanwhile, Qu et al. [2025] employs 3D priors [Xiang et al. 2025] for consistent stylization across views. Crucially, all these approaches follow a style-transfer formulation, requiring a user-provided target shape to define the geometry structure. In contrast, our method addresses a distinct task of reference-guided 3D shape generation. From the reference, rather than extracting explicit geometry, we extract category-agnostic shape concepts that can be composed flexibly with texts to synthesize new shapes, considering the structural semantics in the text, while preserving the learned geometric/appearance attributes from the reference shape.

3D Generative Modeling. Inspired by the success of diffusion models in 2D image and video generation [Ho et al. 2020, 2022], recent works [Cheng et al. 2023; Hu et al. 2024a; Liu et al. 2023a; Ren et al. 2024; Zeng et al. 2022; Zhang et al. 2023b] have significantly advanced 3D generative modeling by learning compact latent representations and performing generation in the compressed space. With the emergence of large-scale 3D datasets [Deitke et al. 2023a,b], 3D foundation models [He et al. 2025; Hong et al. 2025, 2024; Hui et al. 2022; Li et al. 2025; Wu et al. 2024a, 2025b; Xiang et al. 2025; Zhang et al. 2024; Zhao et al. 2025] have been developed to capture strong geometric priors supporting not only high-quality asset generation across diverse categories but also a wide range of downstream tasks, e.g., shape analysis [Du et al. 2025] and editing [Hu et al. 2024b]. Despite their impressive generalization, these models primarily generate samples from a learned distribution and lack mechanisms for user-specified personalization or example-based control. In this work, we leverage the robust priors of the 3D foundation model TRELLIS [Xiang et al. 2025] with a decoupled personalization framework to enable flexible user-specified adaptation

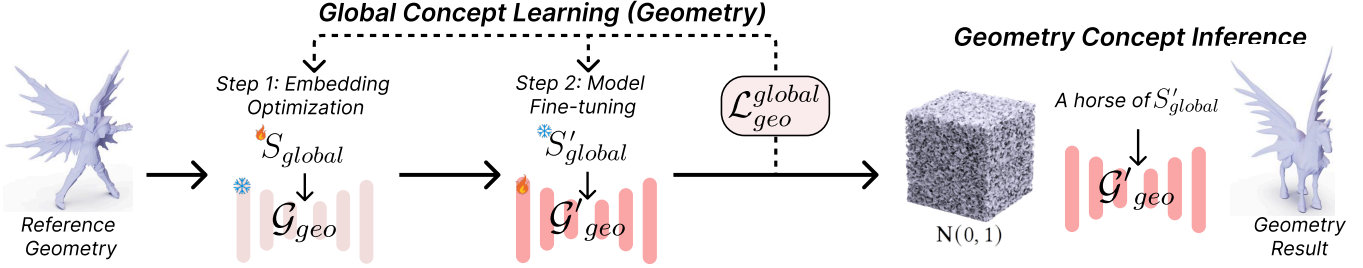


Fig. 2. Global concept learning in PEGAsus. Given a reference shape, we first optimize the text embedding S_{global} to S'_{global} then fine-tune the geometry generator G_{geo} to G'_{geo} ; both steps are guided by the global (geometry) loss $\mathcal{L}_{geo}^{global}$. At inference, we compose the learned concept S'_{global} with a text prompt and use the fine-tuned model to generate new shapes with the inherited reference attributes. This figure shows global concept learning for geometry, yet the same pipeline can be used for appearance, by replacing G_{geo} with the appearance generator and adjusting the reference data from geometry to appearance.

of geometry and appearance, while maintaining the high-quality generative capabilities of the base model.

Image personalization aims to adapt large text-to-image generative models [Rombach et al. 2022] to capture the visual identity of a specific subject or concept from a set of reference images, enabling faithful synthesis under new text prompts. Textual Inversion [Gal et al. 2023] introduces personalization by learning a concept-specific text embedding, whereas DreamBooth [Ruiz et al. 2023] improves the fidelity via model fine-tuning. Subsequent methods [Gu et al. 2023; Kumari et al. 2023; Ruiz et al. 2024; Safaei et al. 2024; Shi et al. 2024; Tewel et al. 2023; Wei et al. 2023; Ye et al. 2023] increase efficiency and controllability by updating only lightweight parameters or leveraging image encoders, and others [Avrahami et al. 2023; Safaei et al. 2024] further extend personalization to spatially localized concepts for fine-grained, compositional control. Despite these advances, direct 3D personalization remains underexplored. Existing works [Huang et al. 2025; Liu et al. 2024; Raj et al. 2023; Wang et al. 2024] propose to lift personalized image diffusion priors into 3D, so the geometry and appearance are entangled, with limited geometric control and weak cross-category generalization. In contrast, we perform personalization directly in 3D, explicitly disentangling geometry- and appearance-level concepts, enabling cross-category concept-level shape generation. Further, we formulate a region-wise mechanism to localize the concept learning.

3 Overview

We develop the shape concept learning pipelines in PEGAsus based on the geometry generator G_{geo} and appearance generator G_{app} of TRELLIS [Xiang et al. 2025]; see Section 4.1. Importantly, we model the shape concept *jointly* by a *learnable text embedding* and a *generator model* fine-tuned from G_{geo} or G_{app} . Below, we first overview the global concept learning pipeline in PEGAsus then introduce how we adapt it for region-wise concept learning.

Figure 2 shows the pipeline for global concept learning. Here, we focus on geometry concept, as appearance concept follows a similar procedure. Given a reference shape, we first adopt a progressive optimization strategy (Section 4.2) to extract a global concept. Then, we optimize the text embedding S_{global} to S'_{global} with a frozen generator (G_{geo} , for the case of geometry concept) to extract coarse global attribute, without disrupting the generator’s prior. Next, we fine-tune generator G_{geo} to G'_{geo} to adapt it to fine-grained attribute

details, while fixing the optimized text embedding S'_{global} . Crucially, both steps employ the same objective $\mathcal{L}_{geo}^{global}$, differing only in the parameters being optimized. At inference, the learned geometry concept embedding S'_{global} can be composed with text and fed into the fine-tuned generator G'_{geo} to synthesize new shapes (Section 4.4).

Figure 3 shows the pipeline for region-wise concept learning. For brevity, we illustrate it with appearance concept, as geometry concept follows analogously. Given a reference shape with a user-specified region, we first extract region-wise concept using the progressive optimization strategy. Then, we adapt the global pipeline by introducing two complementary losses, *i.e.*, context-aware loss \mathcal{L}^{ctx} and context-free loss \mathcal{L}^{free} , to facilitate independent yet coherent region-wise concept learning (Section 4.3). At inference, the learned appearance concept can then be employed to generate shapes with the desired appearance attributes (Section 4.4).

4 Method

4.1 Preliminary: TRELLIS

First, we briefly review TRELLIS [Xiang et al. 2025] for the necessary background. TRELLIS uses a unified *Structured Latent* (SLAT) representation $\{(V, Z) \mid V = \{p_i\}_{i=1}^L, Z = \{z_i\}_{i=1}^L\}$, where V defines the geometry structure via spatial coordinates p_i and Z defines the associated appearance features z_i . This representation decouples the 3D generation into two stages: (i) a sparse structure stage to synthesize V and (ii) a structured latent stage to generate Z .

Stage 1: Sparse Structure Stage. This stage encodes geometry V into a latent voxel grid X using a pre-trained VAE, then trains the geometry generator G_{geo} to denoise X , conditioned on text y :

$$\mathcal{L}_{geo} = \mathbb{E}_{t, X_t, y} [\|v_t - G_{geo}(X_t, t, y)\|^2], \quad (1)$$

where X_t is the noisy latent at time t and v_t is the target velocity. Then, the VAE decoder maps the denoised X to generate V .

Stage 2: Structured Latent Stage. Given the geometry V , the second stage trains the appearance generator G_{app} to denoise $Z = \{z_i\}_{i=1}^L$ from Gaussian noise, conditioned on text y and the fixed V :

$$\mathcal{L}_{app} = \mathbb{E}_{t, Z_t, y, V} [\|u_t - G_{app}(Z_t, t, y, V)\|^2], \quad (2)$$

where Z_t is the noisy latent at time t and u_t is the target velocity. The resulting structured latent (V, Z) can then be decoded into various 3D representations, *e.g.*, 3D Gaussian splats and meshes.

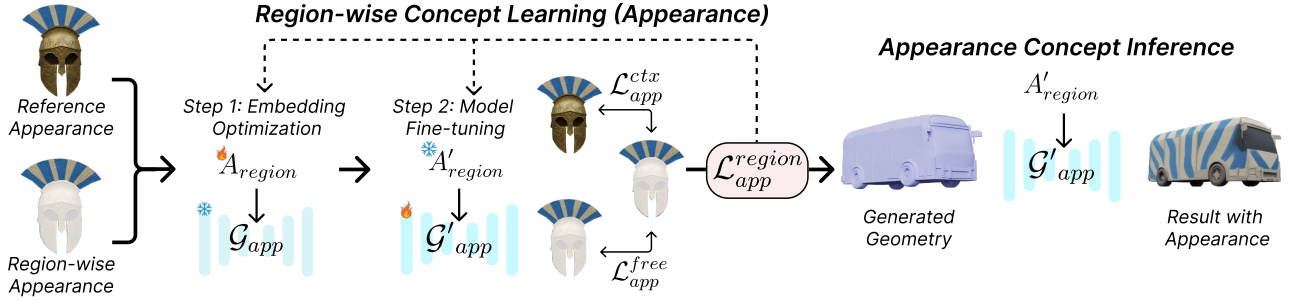


Fig. 3. Region-wise concept learning in PEGAsus. Given a reference appearance with a user-specified region, we perform a progressive optimization strategy with a region-wise (appearance) objective $\mathcal{L}_{app}^{region}$. This objective combines \mathcal{L}_{app}^{ctx} and \mathcal{L}_{app}^{free} to encourage the learned concept to be visually coherent and conceptually independent. At inference, the concept synthesizes result that inherits the attributes of the specified region. While this figure shows region-wise concept learning for appearance, the pipeline applies to geometry by replacing G_{app} with G_{geo} and switching reference data to geometry.

Building on this SLAT representation, we treat geometry and appearance as distinct personalization targets, facilitating decoupled concept learning at both the geometry and appearance levels.

4.2 Global Concept Learning

Fundamentally, 3D personalization involves a trade-off between (i) concept fidelity, *i.e.*, how accurately the concept captures the reference attributes, and (ii) transferability, *i.e.*, how well the concept can be composed with text to generate new shapes. Relying solely on optimizing text embeddings is often insufficient, as the compact text embedding space lacks the capacity to encode detailed geometric or appearance attributes; see an ablation in Figure 7(c). Meanwhile, directly fine-tuning the generator on a single reference shape usually disrupts its 3D priors, leading to overfitting where the fine-tuned model fails to generalize to novel shapes; see Figure 7(d).

Progressive Optimization Strategy. To address the above issues, we formulate the progressive optimization strategy to optimize the joint shape concept, *i.e.*, a text embedding and a generator model. Below, we denote \mathcal{G} as the generator, \mathcal{D} the reference shape representation, and C a learnable text embedding initialized from a neutral text description, *e.g.*, “object”, encoded by CLIP [Radford et al. 2021].

- **Step 1: Embedding Optimization.** We first capture coarse global attributes by optimizing only the text embedding. Since the text embedding C is initialized from a neutral word, we utilize a relatively high learning rate to optimize it to C' while freezing the generator \mathcal{G} . This encourages the generic text embedding to align with the coarse global structure \mathcal{D} without altering the generative prior.
- **Step 2: Model Fine-tuning.** To recover fine-grained details that the embedding alone cannot represent, we fix the optimized text embedding C' and fine-tune generator \mathcal{G} to \mathcal{G}' using a low learning rate. This conservative update alleviates overfitting to the single reference instance while allowing the model to capture high-frequency details of \mathcal{D} that were missed in the embedding optimization step.

Crucially, while the two steps have different optimization parameters, the objective function remains identical. Below, we specify the reference data \mathcal{D} , the learnable text embedding C , the generator \mathcal{G} , and the objective function for each case of concept learning.

Global Geometry Concept Learning. For geometry concept learning, we construct the reference shape \mathcal{D} by first voxelizing the reference shape, and encoding the voxel grid into the latent feature grid X . Then, we initialize the learnable text embedding C as S_{global} and optimize it to S'_{global} . We set the generator \mathcal{G} as \mathcal{G}_{geo} , adopt the same flow matching objective as Equation 1, but replace the standard text condition y with our learnable text embedding S_{global} :

$$\mathcal{L}_{geo}^{global} = \mathbb{E}_{t, X_t} [||v_t - \mathcal{G}_{geo}(X_t, t, S_{global})||^2]. \quad (3)$$

Global Appearance Concept Learning. We define the appearance reference \mathcal{D} as the SLAT representation (V, Z) extracted from the reference shape, following TRELLIS [Xiang et al. 2025], where Z serves as the target appearance features and V as the fixed geometry condition. We set the generator \mathcal{G} as \mathcal{G}_{app} , initialize the learnable text embedding C as A_{global} , and then optimize it to A'_{global} . The global appearance loss follows Equation 2, but replacing the text prompt y with the appearance text embedding A_{global} :

$$\mathcal{L}_{app}^{global} = \mathbb{E}_{t, Z_t, V} [||u_t - \mathcal{G}_{app}(Z_t, t, A_{global}, V)||^2]. \quad (4)$$

The final learned concept is jointly represented by the optimized embedding and the fine-tuned generator: $(S'_{global}, \mathcal{G}'_{geo})$ for global geometry concept and $(A'_{global}, \mathcal{G}'_{app})$ for global appearance concept.

4.3 Region-wise Concept Learning

While global concept learning effectively captures the overall attributes of a reference shape, it lacks the precision to extract concepts from a specific local region. To enhance user controllability and enable more flexible personalization, we introduce region-wise concept learning, which enables the extraction of geometry and appearance concepts from a user-specified region. Given a reference shape \mathcal{D} and a mask M denoting a user-specified region, we learn a region-wise shape concept $(C_{region}, \mathcal{G})$, to capture the attributes within M . To achieve this, we employ the same progressive optimization strategy proposed in the Section 4.2.

However, a challenge in region-wise concept learning is balancing context awareness with concept independence. When optimizing using the full reference shape as input while restricting supervision solely to the masked region, the generator tends to exploit the surrounding context to infer the masked region. This leads to entanglement, where the learned concept relies on the global shape

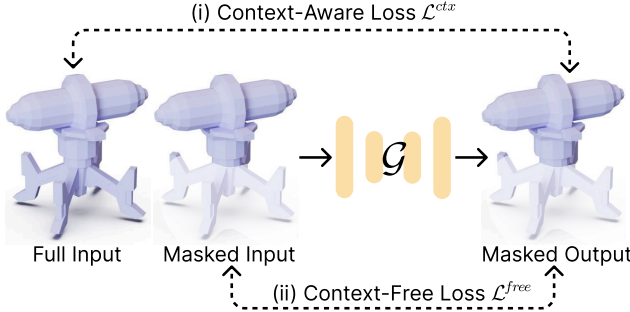


Fig. 4. Region-wise concept learning objectives. (i) Context-Aware Loss \mathcal{L}^{ctx} takes full reference and computes loss within the masked region. (ii) Context-Free Loss uses masked input to calculate loss within the masked region.

rather than being an independent attribute. Conversely, if we strictly isolate the region by masking out the rest of the shape, the concept may lose its semantic coherence with the global geometry. To address this trade-off, we introduce two complementary losses:

- Context-Aware Loss (\mathcal{L}^{ctx}). As shown in Figure 4(i), we feed the full reference shape to the generator but calculate the loss only within the mask M . The localized supervision constrains the optimization to the masked region while leveraging the global context of the reference shape. This encourages the concept to maintain the semantic coherence between the masked region and the global structure.
- Context-Free Loss (\mathcal{L}^{free}). As shown in Figure 4(ii), we mask the user-specified region of the reference shape before feeding it into the generator. By requiring the model to reconstruct the masked region in the absence of surrounding context, we encourage the learned concept to be isolated from its neighbors and thus conceptually independent.

Below, we instantiate this region-wise concept learning framework for both geometry and appearance concepts.

Region-wise Geometry Concept Learning. For geometry, the reference data \mathcal{D} refers to a latent feature grid X , obtained by encoding the voxelized reference shape. Given a binary voxel mask M , we downsample it to align with the latent feature grid resolution, obtaining M_{geo} . We initialize the text embedding C_{region} as S_{region} and the generator \mathcal{G} as \mathcal{G}_{geo} . The specific losses are defined as:

$$\mathcal{L}_{geo}^{ctx} = \mathbb{E}_{t, X_t} [\| M_{geo} \odot (v_t - \mathcal{G}_{geo}(X_t, t, S_{region})) \|^2] \quad (5)$$

$$\text{and } \mathcal{L}_{geo}^{free} = \mathbb{E}_{t, X_t^M} [\| M_{geo} \odot (v_t - \mathcal{G}_{geo}(X_t^M, t, S_{region})) \|^2], \quad (6)$$

where X_t is the noisy grid derived from the latent X of the full reference shape, and X_t^M is derived from the latent X^M encoded from the masked reference shape.

$$\mathcal{L}_{geo}^{region} = \mathcal{L}_{geo}^{ctx} + \lambda_1 \mathcal{L}_{geo}^{free} \quad (7)$$

Region-wise Appearance Concept Learning. For appearance, we define the reference data as the SLAT representation $\mathcal{D} = (V, Z)$. Given a region specified by the user, we define a binary mask M_{app} on the sparse voxels V . We initialize the text embedding C_{region} as A_{region} and the generator \mathcal{G} as \mathcal{G}_{app} with the following objectives:

$$\mathcal{L}_{app}^{ctx} = \mathbb{E}_{t, Z_t, V} [\| M_{app} \odot (u_t - \mathcal{G}_{app}(Z_t, t, A_{region}, V)) \|^2] \quad (8)$$



Fig. 5. Our method supports extracting concepts from global geometry, region-wise geometry, global appearance, and region-wise appearance, and composing the learned concepts with text to generate novel shapes.

and

$$\mathcal{L}_{app}^{free} = \mathbb{E}_{t, Z_t^M, V^M} [\| M_{app} \odot (u_t - \mathcal{G}_{app}(Z_t^M, t, A_{region}, V^M)) \|^2], \quad (9)$$

where Z_t^M denotes the noisy latents derived from the masked appearance features $Z \odot M_{app}$, and $V^M = V \odot M_{app}$ represents the masked geometry containing only voxels within the masked region. The total region-wise appearance objective is defined as:

$$\mathcal{L}_{app}^{region} = \mathcal{L}_{app}^{ctx} + \lambda_2 \mathcal{L}_{app}^{free}. \quad (10)$$

The learned concept is represented by an optimized embedding and a fine-tuned generator: $(S'_{region}, \mathcal{G}'_{geo})$ for region-wise geometry concept and $(A'_{region}, \mathcal{G}'_{app})$ for region-wise appearance concept.

4.4 Shape Concept Inference

The learned concepts serve as reusable components during inference. By leveraging the decoupled designs of geometry and appearance concepts, our framework allows them to be applied independently, enabling flexible personalization with fine-grained control. Below, we describe the concept inference for geometry and appearance.

Geometry Concept Inference. We employ the learned geometry concept (S', \mathcal{G}'_{geo}) to synthesize new 3D shapes. Specifically, we construct a target text prompt y_{target} by combining the learned text embedding S' with new text prompts and feed the y_{target} into the fine-tuned generator \mathcal{G}'_{geo} to produce a novel shape. By leveraging the geometric attributes encoded in (\mathcal{G}'_{geo}, S') , we can produce a shape follows the semantic controls of the text prompt while inheriting the geometric attributes of the reference shape.

Appearance Concept Inference. Given a generated geometry V , we employ the learned appearance concept (A', \mathcal{G}'_{app}) to synthesize its

Table 1. Quantitative comparisons for geometry concept. Our method surpasses existing baselines across all quantitative metrics and user study results, demonstrating the effectiveness of our approach.

Method	KID \downarrow	CLIP-R \uparrow	QS \uparrow	AS \uparrow	TS \uparrow
Qwen-Edit [Wu et al. 2025a]	0.0088	0.778	3.87	3.13	3.62
Edit360 [Huang et al. 2025]	0.0082	0.644	3.43	2.44	3.53
Coin3D [Dong et al. 2024]	0.0176	0.544	2.45	1.81	2.39
VoxHammer [Li et al. 2026]	0.0094	0.200	3.44	4.11	1.23
StyleSculptor [Qu et al. 2025]	0.0197	0.589	3.88	1.30	4.27
Ours	0.0064	0.833	4.41	4.15	4.31

Table 2. Quantitative comparisons for appearance concept. Our method outperforms all baselines in both attribute preservation and overall visual quality, as demonstrated by both metric evaluations and user studies.

Method	ArtFID \downarrow	FID \downarrow	QS \uparrow	MS \uparrow
Paint3D [Zeng et al. 2024]	29.16	280.5	3.42	2.91
StyleTex [Xie et al. 2024]	30.42	266.5	2.76	2.25
StyleSculptor [Qu et al. 2025]	27.50	258.5	3.25	2.92
Ours	23.45	235.9	4.67	4.37

appearance. The fine-tuned appearance generator \mathcal{G}'_{app} produces the appearance latent Z , conditioned on the geometry V and the appearance text embedding A' . Finally, the structured latents (V, Z) are decoded into a final 3D asset. By utilizing the appearance attributes encoded within (A', \mathcal{G}'_{app}) , the produced 3D asset maintains an appearance that is consistent with the original reference.

Geometry/Appearance Concepts Composition. As Figures 1 and 5 show, we support composing learned geometry and appearance concepts, learned from either global or region-wise mechanism, to synthesize new shapes. We first apply the learned geometry concept composed with the text prompt to generate the shape geometry. Then, we apply the appearance concept with the generated geometry to synthesize its appearance. This design enables flexible concepts composition and provides users with fine-grained controllability.

5 Results and Experiments

5.1 Experiment Settings

To evaluate the effectiveness of our method, we compare it with various baselines for both geometry and appearance concepts.

Geometry Concept. To evaluate our method under this new task, we conduct a comprehensive evaluation by adapting five representative methods from closely related fields: (i) Qwen-Edit [Wu et al. 2025a], (ii) Edit360 [Huang et al. 2025], (iii) StyleSculptor [Qu et al. 2025], (iv) Coin3D [Dong et al. 2024], and (v) VoxHammer [Li et al. 2026]. Qwen-Edit and Edit360 perform image personalization followed by 3D reconstruction [Wang et al. 2021; Xiang et al. 2025]. VoxHammer targets text-guided shape editing, whereas Coin3D combines coarse geometric proxies with text for generation. StyleSculptor requires a target shape for 3D stylization; we generate it from text using TRELLIS. For a comprehensive evaluation, we introduce a benchmark of 30 reference shapes from Objaverse-XL [Deitke et al. 2023a]. Each reference is paired with three distinct text prompts targeting different categories, establishing a total of 90 evaluation cases. More details about the geometry concept benchmark are provided in supplementary Section A.1.

Appearance Concept. To evaluate our method for the new appearance concept task, we perform a comprehensive evaluation against three methods adapted from closely related fields: (i) Paint3D [Zeng et al. 2024], (ii) StyleTex [Xie et al. 2024], and (iii) StyleSculptor [Qu et al. 2025]. Since Paint3D and StyleTex apply appearance from an image to a shape, we adapt them by rendering the reference appearance shape into an input image. For StyleSculptor, it requires source and target images, so we render both the reference appearance shape and the geometry shape. For a fair evaluation, we constructed a benchmark of 30 pairs from Objaverse-XL [Deitke et al. 2023a], where each pair consists of a reference appearance shape and a geometry shape. More details about the appearance concept benchmark are provided in supplementary Section A.2.

5.2 Quantitative Comparison

Evaluation Metrics. To evaluate geometry concept, we first assess the visual quality of the generated shapes using Kernel Inception Distance (KID). Following [Liu et al. 2024; Raj et al. 2023], we utilize CLIP R-Precision (CLIP-R) to evaluate the text alignment. For appearance concept, we adopt ArtFID [Wright and Ommer 2022] to assess appearance fidelity between the reference and generated results. Then, we follow [Qu et al. 2025] to use Fréchet Inception Distance (FID) to measure the visual quality of the generated appearance.

User Study. Following [Hu* et al. 2023; Hu et al. 2024b], we conducted a user study with 10 participants to evaluate geometry and appearance concepts. Participants rated results on a Likert scale from 0 (worst) to 5 (best). For geometry, evaluations focused on: (i) Quality Score (QS), reflecting visual quality; (ii) Attribute Score (AS), assessing the preservation of geometric attributes; and (iii) Text Score (TS), evaluating how well the generated shapes follow the text. For appearance, participants evaluated: (i) Quality Score (QS); and (ii) Matching Score (MS), measuring the similarity between the generated appearance and the reference.

Table 1 presents the quantitative results for geometry concept. Across all metrics, our method outperforms prior approaches: it produces higher-quality geometry (higher QS, lower KID), better preserves reference attributes (higher CLIP-R, AS), and follows text control more faithfully (higher CLIP-R, TS). Table 2 reports the results for appearance concept. Our method achieves the best performance, with stronger appearance preservation (lower ArtFID, higher MS) and higher-quality generations (lower FID, higher QS).

5.3 Qualitative Comparison

Geometry Concept. Figure 8 presents visual comparisons for the geometry concept. As shown in second row, our method can produce results that preserve geometric attributes, e.g., vertical slats, while adhere to the text control. In contrast, baselines either discard geometric attributes or fail to match the text.

Appearance Concept. Figure 9 provides visual comparisons for appearance concept. Our method better preserves the appearance attribute of the reference than baselines. As shown in row 1 (left), our method retains the bridge’s blue and black pattern, whereas others alter the color distribution.

More comparisons are showed in supplementary Sections B & C.

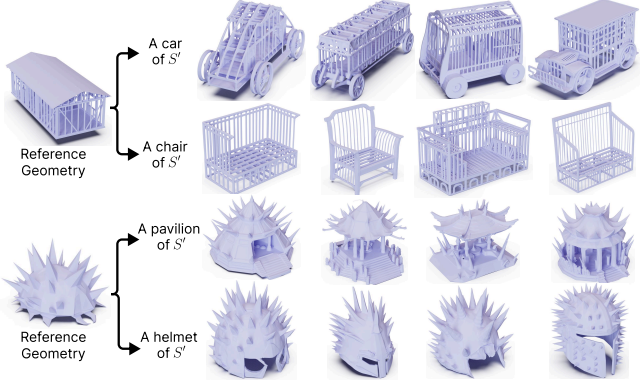


Fig. 6. Visual results for global geometry concept variations. Our method generates diverse shapes that preserve the same geometric attributes, e.g., vertical slats or spikes, while consistently following the same text controls.

5.4 More Visual Results

We provide additional visual results for our method. We first present results for the global geometry concept: Figure 6 illustrates the visual result for concept-level shape variations with the same text, while Figure 10 demonstrates the synthesis of novel shapes using different text prompts. Next, Figure 11 displays results for the global appearance concept. We then show results for region-wise concept: Figure 12 provides additional visualizations for region-wise geometry concept, and Figure 13 presents visual results of the region-wise appearance concept. More visual results are provided in supplementary material Sections D, E, F, and G.

5.5 Ablation Study

We first perform ablation to validate progressive optimization strategy. When relying solely on embedding optimization, the method struggles to capture fine-grained geometric and appearance attributes. As Figure 7(c) shows, it fails to preserve the geometric attributes and generates a generic robot. For appearance, it cannot reproduce the black-and-white pattern, resulting in a generic giraffe-like texture. Yet, using only model fine-tuning causes the model to overfit and lose text control. As Figure 7(d) demonstrates, the geometry fails to follow the text control, while the appearance mimics white colors rather than the black-white patterns. In contrast, our full pipeline effectively balances these trade-offs, ensuring both attribute preservation and text control; see Figure 7(b).

We next ablate the two complementary losses in our region-wise objective. First, we remove the context-aware loss \mathcal{L}^{ctx} for ablation. As shown in Figure 7(g), removing \mathcal{L}^{ctx} degrades visual coherency. While the geometry concept captures vertical slats, it appears fragmented, and the appearance concept fails to retain the pink-and-white pattern. Second, removing \mathcal{L}^{free} makes the model fail to preserve attributes. As Figure 7(h) shows, geometry is generated solely by the text while generated appearance struggles to maintain the pink-and-white pattern.

Table 3 shows quantitative ablation studies. Removing either embedding optimization or model fine-tuning hinders both geometry and appearance concept learning.

Table 3. Quantitative comparison of our full pipeline against ablated cases.

Method	Geometry		Appearance	
	KID ↓	CLIP-R ↑	ArtFID ↓	FID ↓
Ours w/o Embedding Opt.	0.0075	0.567	29.21	276.03
Ours w/o Model Fine-tuning	0.0117	0.489	31.82	302.76
Full pipeline	0.0064	0.842	23.45	235.9

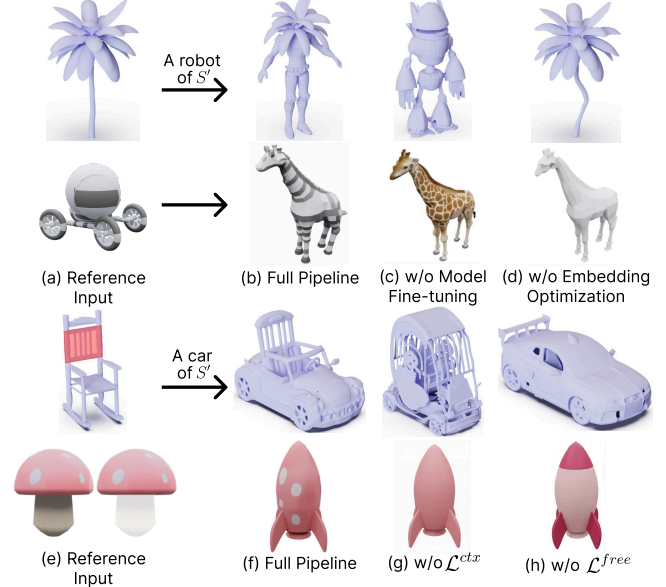


Fig. 7. Visual results for the ablation studies. (c) Removing model fine-tuning weakens attribute capture, while (d) removing embedding optimization leads to overfitting. For region-wise learning, (g) removing context-aware loss reduces visual coherence, whereas (h) removing the context-free loss hinders the model from capturing the reference attributes.

6 Conclusions

We have presented a notion of 3D personalization that shifts the focus from instance-level control to concept-level abstraction. Rather than cloning, deforming, or editing a reference shape, our approach treats personalization as the extraction of reusable geometric and appearance concepts that can be recomposed across categories. This formulation departs from target-driven pipelines that operate by modifying an existing shape, and instead enables reference-guided generation without prescribing any target instance. Conceptually, this places 3D personalization closer to language-level creativity, where abstract attributes are learned from examples and flexibly combined with semantic intent, rather than framing it as yet another geometry editing or localized shape manipulation technique. By operating at transferable concept level, the method supports a more compositional and open-ended paradigm for 3D content creation.

Building on this notion, we showed that framing personalization around concept extraction leads to a more compositional view of 3D generation. Concepts could be learned at different scales, extracted locally or globally, and combined with one another and with text in a flexible manner. Rather than producing a single edited result, this opens the door to more modular and expressive ways of creating

3D content, where new designs can emerge from the reuse and recombination of learned ideas.

References

- Omri Avrahami, Kfir Aberman, Ohad Fried, Daniel Cohen-Or, and Dani Lischinski. 2023. Break-A-Scene: Extracting Multiple Concepts from a Single Image. In *Proceedings of SIGGRAPH Asia*. 1–12.
- Martin Bokeloh, Michael Wand, and Hans-Peter Seidel. 2010. A Connection between Partial Symmetry and Inverse Procedural Modeling. *ACM Transactions on Graphics (SIGGRAPH)* (2010), 1–10.
- Siddhartha Chaudhuri, Evangelos Kalogerakis, Leonidas Guibas, and Vladlen Koltun. 2011. Probabilistic Reasoning for Assembly-based 3D Modeling. *ACM Transactions on Graphics (SIGGRAPH)* (2011), 1–10.
- Qimin Chen, Yuezhi Yang, Yifang Wang, Vladimir G. Kim, Siddhartha Chaudhuri, Hao Zhang, and Zhiqin Chen. 2025. ART-DECO: Arbitrary Text Guidance for 3D Detailizer Construction. In *Proceedings of SIGGRAPH Asia*. 1–12.
- Yen-Chi Cheng, Hsin-Ying Lee, Sergey Tulyakov, Alexander G Schwing, and Liang-Yan Gui. 2023. SDFusion: Multimodal 3D Shape Completion, Reconstruction, and Generation. In *IEEE Conference on Computer Vision and Pattern Recognition (CVPR)*. 4456–4465.
- Matt Deitke, Ruoshi Liu, Matthew Wallingford, Huong Ngo, Oscar Michel, Aditya Kusupati, Alan Fan, Christian Laforte, Vikram Voleti, Samir Yitzhak Gadre, et al. 2023a. Objaverse-XL: A Universe of 10M+ 3D Objects. *arXiv preprint arXiv:2307.05663* (2023).
- Matt Deitke, Dustin Schwenk, Jordi Salvador, Luca Weihs, Oscar Michel, Eli VanderBilt, Ludwig Schmidt, Kiana Ehsani, Aniruddha Kembhavi, and Ali Farhadi. 2023b. Objaverse: A Universe of Annotated 3D Objects. In *IEEE Conference on Computer Vision and Pattern Recognition (CVPR)*. 13142–13153.
- Wenqi Dong, Bangbang Yang, Lin Ma, Xiao Liu, Liyuan Cui, Hujun Bao, Yuewen Ma, and Zhaopeng Cui. 2024. Coin3D: Controllable and Interactive 3D Assets Generation with Proxy-Guided Conditioning. In *Proceedings of SIGGRAPH*. 1–12.
- Keyu Du, Jingyu Hu, Haipeng Li, Hao Xu, Haibin Huang, Chi-Wing Fu, and Shuaicheng Liu. 2025. Hierarchical neural semantic representation for 3d semantic correspondence. In *Proceedings of SIGGRAPH Asia*. 1–11.
- Zhiwen Fan, Yifan Jiang, Peihao Wang, Xinyu Gong, Dejia Xu, and Zhangyang Wang. 2022. Unified Implicit Neural Stylization. In *European Conference on Computer Vision (ECCV)*.
- Matthew Fisher, Daniel Ritchie, Manolis Savva, Thomas Funkhouser, and Pat Hanrahan. 2012. Example-based Synthesis of 3D Object Arrangements. *ACM Transactions on Graphics* 31, 6 (2012), 1–11.
- Thomas Funkhouser, Michael Kazhdan, Philip Shilane, Patrick Min, William Kiefer, Ayellet Tal, Szymon Rusinkiewicz, and David Dobkin. 2004. Modeling by Example. *ACM Transactions on Graphics* 23, 3 (2004), 652–663.
- Rinon Gal, Yuval Alaluf, Yuval Atzmon, Or Patashnik, Amit H Bermano, Gal Chechik, and Daniel Cohen-Or. 2023. An Image is Worth One Word: Personalizing Text-to-Image Generation using Textual Inversion. In *International Conference on Learning Representations (ICLR)*.
- Yuchao Gu, Xiantao Wang, Jay Zhangjie Wu, Yujun Shi, Yunpeng Chen, Zihan Fan, Wuyou Xiao, Rui Zhao, Shuning Chang, Weijia Wu, et al. 2023. Mix-of-Show: Decentralized Low-Rank Adaptation for Multi-Concept Customization of Diffusion Models. In *Conference on Neural Information Processing Systems (NeurIPS)*. 15890–15902.
- Xianglong He, Zi-Xin Zou, Chia-Hao Chen, Yuan-Chen Guo, Ding Liang, Chun Yuan, Wanli Ouyang, Yan-Pei Cao, and Yangguang Li. 2025. SparseFlex: High-Resolution and Arbitrary-Topology 3D Shape Modeling. In *IEEE International Conference on Computer Vision (ICCV)*.
- Amir Hertz, Rana Hanocka, Raja Giryes, and Daniel Cohen-Or. 2020. Deep Geometric Texture Synthesis. *ACM Transactions on Graphics (SIGGRAPH)* 39, 4 (2020), 1–11.
- Jonathan Ho, Ajay Jain, and Pieter Abbeel. 2020. Denoising Diffusion Probabilistic Models. *Conference on Neural Information Processing Systems (NeurIPS)* (2020), 6840–6851.
- Jonathan Ho, Tim Salimans, Alexey Grigchenko, William Chan, Mohammad Norouzi, and David J Fleet. 2022. Video Diffusion Models. In *Conference on Neural Information Processing Systems (NeurIPS)*. 8633–8646.
- Lukas Höller, Justin Johnson, and Matthias Nießner. 2022. StyleMesh: Style Transfer for Indoor 3D Scene Reconstructions. In *IEEE Conference on Computer Vision and Pattern Recognition (CVPR)*. 6198–6208.
- Fangzhou Hong, Jiaxiang Tang, Ziang Cao, Min Shi, Tong Wu, Zhaoxi Chen, Tengfei Wang, Liang Pan, Dahua Lin, and Ziwei Liu. 2025. 3DTopia-XL: Scaling High-quality 3D Asset Generation via Primitive Diffusion. In *IEEE Conference on Computer Vision and Pattern Recognition (CVPR)*.
- Yicong Hong, Kai Zhang, Juxiang Gu, Sai Bi, Yang Zhou, Difan Liu, Feng Liu, Kalyan Sunkavalli, Trung Bui, and Hao Tan. 2024. LRM: Large Reconstruction Model for Single Image to 3D. (2024).
- Jingyu Hu, Ka-Hei Hui, Chi-Wing Fu, and Zhengzhe Liu. 2024a. Neural Wavelet-Domain Diffusion for 3D Shape Generation, Inversion, and Manipulation. *ACM Transactions on Graphics* 42, 6 (2024).
- Jingyu Hu*, Ka-Hei Hui*, Zhengzhe Liu, Hao Zhang, and Chi-Wing Fu. 2023. CLIPX-Plore: Coupled CLIP and Shape Spaces for 3D Shape Exploration. In *Proceedings of SIGGRAPH Asia*. 1–12.
- Jingyu Hu, Ka-Hei Hui, Zhengzhe Liu, Hao Zhang, and Chi-Wing Fu. 2024b. CNS-Edit: 3D Shape Editing via Coupled Neural Shape Optimization. In *ACM SIGGRAPH 2024 Conference Papers*. 1–12.
- Ruizhen Hu, Wenchao Li, Oliver Van Kaick, Hui Huang, Melinos Averkiou, Daniel Cohen-Or, and Hao Zhang. 2017. Co-Locating Style-Defining Elements on 3D Shapes. *ACM Transactions on Graphics* 36, 3 (2017), 1–15.
- Hsin-Ping Huang, Hung-Yu Tseng, Saurabh Saini, Maneesh Singh, and Ming-Hsuan Yang. 2021. Learning to Stylize Novel Views. In *IEEE Conference on Computer Vision and Pattern Recognition (CVPR)*. 13869–13878.
- Junchao Huang, Xinting Hu, Zhuotao Tian, Shaoshuai Shi, and Li Jiang. 2025. Edit360: 2D Image Edits to 3D Assets from Any Angle. In *Proceedings of the IEEE/CVF International Conference on Computer Vision (ICCV)*.
- Yi-Hua Huang, Yue He, Yu-Jie Yuan, Yu-Kun Lai, and Lin Gao. 2022. StylizedNeRF: Consistent 3D Scene Stylization as Stylized NeRF via 2D–3D Mutual Learning. In *IEEE Conference on Computer Vision and Pattern Recognition (CVPR)*. 18342–18352.
- Ka-Hei Hui, Ruihui Li, Jingyu Hu, and Chi-Wing Fu. 2022. Neural Wavelet-domain Diffusion for 3D Shape Generation. In *Proceedings of SIGGRAPH Asia*. 1–9.
- Evangelos Kalogerakis, Siddhartha Chaudhuri, Daphne Koller, and Vladlen Koltun. 2012. A Probabilistic Model for Component-based Shape Synthesis. *ACM Transactions on Graphics (SIGGRAPH)* 31, 4 (2012), 1–11.
- Hiroharu Kato, Yoshitaka Ushiku, and Tatsuya Harada. 2018. Neural 3D Mesh Renderer. In *IEEE Conference on Computer Vision and Pattern Recognition (CVPR)*. 3907–3916.
- Moneish Kumar, Neeraj Panse, and Dishani Lahiri. 2023. S2RF: Semantically Stylized Radiance Fields. In *IEEE Conference on Computer Vision and Pattern Recognition (CVPR)*. 2952–2957.
- Nupur Kumar, Bingliang Zhang, Richard Zhang, Eli Shechtman, and Jun-Yan Zhu. 2023. Multi-Concept Customization of Text-to-Image Diffusion. In *IEEE Conference on Computer Vision and Pattern Recognition (CVPR)*. 1931–1941.
- Honghua Li, Hao Zhang, Yanzhen Wang, Junjie Cao, Ariel Shamir, and Daniel Cohen-Or. 2013. Curve Style Analysis in a Set of Shapes. *Computer Graphics Forum* 32, 6 (2013), 77–88.
- Lin Li, Zehuan Huang, Haoran Feng, Gengxiang Zhuang, Rui Chen, Chunhao Guo, and Lu Sheng. 2026. VoxHammer: Training-Free Precise and Coherent 3D Editing in Native 3D Space. In *Proceedings of the IEEE International Conference on 3D Vision (3DV)*.
- Weiyu Li, Xuelin Chen, Jue Wang, and Baoquan Chen. 2023. Patch-based 3D Natural Scene Generation from a Single Example. In *IEEE Conference on Computer Vision and Pattern Recognition (CVPR)*. 16762–16772.
- Yangguang Li, Zi-Xin Zou, Zexiang Liu, Dehu Wang, Yuan Liang, Zhipeng Yu, Xingchao Liu, Yuan-Chen Guo, Ding Liang, Wanli Ouyang, et al. 2025. TripoSG: High-Fidelity 3D Shape Synthesis using Large-Scale Rectified Flow Models. *arXiv preprint arXiv:2502.06608* (2025).
- Fangfu Liu, Hanyang Wang, Weiliang Chen, Haowen Sun, and Yueqi Duan. 2024. Make-Your-3D: Fast and Consistent Subject-Driven 3D Content Generation. In *European Conference on Computer Vision (ECCV)*. 389–406.
- Kunhao Liu, Fangneng Zhan, Yiwen Chen, Jiahui Zhang, Yingchen Yu, Abdulmotaleb El Saddik, Shijian Lu, and Eric P. Xing. 2023b. StyleRF: Zero-Shot 3D Style Transfer of Neural Radiance Fields. In *IEEE Conference on Computer Vision and Pattern Recognition (CVPR)*. 8338–8348.
- Zhengze Liu, Jingyu Hu, Ka-Hei Hui, Xiaojuan Qi, Daniel Cohen-Or, and Chi-Wing Fu. 2023a. EXIM: A Hybrid Explicit-Implicit Representation for Text-Guided 3D Shape Generation. *ACM Transactions on Graphics (SIGGRAPH Asia)* 42, 6 (2023), 1–12.
- Nissim Maruani, Wang Yifan, Matthew Fisher, Pierre Alliez, and Mathieu Desbrun. 2025. ShapeShifter: 3D Variations Using Multiscale and Sparse Point-Voxel Diffusion. In *IEEE Conference on Computer Vision and Pattern Recognition (CVPR)*. 605–617.
- Paul Merrell. 2007. Example-based Model Synthesis. In *Proceedings of the 2007 Symposium on Interactive 3D Graphics and Games*. 105–112.
- Paul Merrell and Dinesh Manocha. 2008. Continuous Model Synthesis. In *ACM SIGGRAPH Asia 2008 papers*. 1–7.
- Oscar Michel, Roi Bar-On, Richard Liu, Sagie Benaim, and Rana Hanocka. 2022. Text2Mesh: Text-Driven Neural Stylization for Meshes. In *IEEE Conference on Computer Vision and Pattern Recognition (CVPR)*. 13492–13502.
- Thu Nguyen-Phuoc, Feng Liu, and Lei Xiao. 2022. SNeRF: Stylized Neural Implicit Representations for 3D Scenes. *ACM Transactions on Graphics (SIGGRAPH)* 41, 6 (2022), 1–11.
- Zefan Qu, Zhenwei Wang, Haoyuan Wang, Ke Xu, Gerhard Hancke, and Rynson W. H. Lau. 2025. StyleSculptor: Zero-Shot Style-Controllable 3D Asset Generation with Texture–Geometry Dual Guidance. In *Proceedings of SIGGRAPH Asia*. 1–12.

- Alec Radford, Jong Wook Kim, Chris Hallacy, Aditya Ramesh, Gabriel Goh, Sandhini Agarwal, Girish Sastry, Amanda Askell, Pamela Mishkin, Jack Clark, et al. 2021. Learning Transferable Visual Models From Natural Language Supervision. In *Proceedings of International Conference on Machine Learning (ICML)*. 8748–8763.
- Amit Raj, Srinivas Kaza, Ben Poole, Michael Niemeyer, Nataniel Ruiz, Ben Mildenhall, Shiran Zada, Kfir Aberman, Michael Rubinstein, Jonathan Barron, et al. 2023. Dream-Booth3D: Subject-Driven Text-to-3D Generation. In *IEEE Conference on Computer Vision and Pattern Recognition (CVPR)*. 2349–2359.
- Xuanchi Ren, Jiahui Huang, Xiaohui Zeng, Ken Museth, Sanja Fidler, and Francis Williams. 2024. XCube: Large-Scale 3D Generative Modeling using Sparse Voxel Hierarchies. In *IEEE Conference on Computer Vision and Pattern Recognition (CVPR)*. 4209–4219.
- Robin Rombach, Andreas Blattmann, Dominik Lorenz, Patrick Esser, and Björn Ommer. 2022. High-Resolution Image Synthesis with Latent Diffusion Models. In *IEEE Conference on Computer Vision and Pattern Recognition (CVPR)*. 10684–10695.
- Nataniel Ruiz, Yuanzhen Li, Varun Jampani, Yael Pritch, Michael Rubinstein, and Kfir Aberman. 2023. DreamBooth: Fine Tuning Text-to-Image Diffusion Models for Subject-Driven Generation. In *IEEE Conference on Computer Vision and Pattern Recognition (CVPR)*. 22500–22510.
- Nataniel Ruiz, Yuanzhen Li, Varun Jampani, Wei Wei, Tingbo Hou, Yael Pritch, Neal Wadhwa, Michael Rubinstein, and Kfir Aberman. 2024. HyperDreamBooth: Hyper-Networks for Fast Personalization of Text-to-Image Models. In *IEEE Conference on Computer Vision and Pattern Recognition (CVPR)*. 6527–6536.
- Mehdi Safaei, Aryan Mikaeili, Or Patashnik, Daniel Cohen-Or, and Ali Mahdavi-Amiri. 2024. CLiC: Concept Learning in Context. In *IEEE Conference on Computer Vision and Pattern Recognition (CVPR)*. 6924–6933.
- Jing Shi, Wei Xiong, Zhe Lin, and Hyun Joon Jung. 2024. InstantBooth: Personalized Text-to-Image Generation without Test-Time Finetuning. In *IEEE Conference on Computer Vision and Pattern Recognition (CVPR)*. 8543–8552.
- Yoad Tewel, Rinon Gal, Gal Chechik, and Yuval Atzmon. 2023. Key-locked Rank One Editing for Text-to-Image Personalization. In *Proceedings of SIGGRAPH*. 1–11.
- Peng Wang, Lingji Liu, Yuan Liu, Christian Theobalt, Taku Komura, and Wenping Wang. 2021. NeuS: Learning Neural Implicit Surfaces by Volume Rendering for Multi-view Reconstruction. In *Conference on Neural Information Processing Systems (NeurIPS)*.
- Zhenwei Wang, Tengfei Wang, Gerhard Hancke, Ziwei Liu, and Rynson W.H. Lau. 2024. ThemeStation: Generating Theme-Aware 3D Assets from Few Exemplars. In *Proceedings of SIGGRAPH*. 1–12.
- Yuxiang Wei, Yabo Zhang, Zhilong Ji, Jinfeng Bai, Lei Zhang, and Wangmeng Zuo. 2023. ELITE: Encoding Visual Concepts into Textual Embeddings for Customized Text-to-Image Generation. In *IEEE Conference on Computer Vision and Pattern Recognition (CVPR)*. 15943–15953.
- Matthias Wright and Björn Ommer. 2022. ArtFID: Quantitative Evaluation of Neural Style Transfer. In *DAGM German Conference on Pattern Recognition*. 560–576.
- Chenfei Wu, Jiahao Li, Jingren Zhou, Junyang Lin, Kaiyuan Gao, Kun Yan, Sheng-ming Yin, Shuai Bai, Xiao Xu, Yilei Chen, et al. 2025a. Qwen-Image Technical Report. *arXiv preprint arXiv:2508.02324* (2025).
- Rundi Wu, Ruoshi Liu, Carl Vondrick, and Changxi Zheng. 2024b. Sin3DM: Learning a Diffusion Model from a Single 3D Textured Shape. In *International Conference on Learning Representations (ICLR)*.
- Rundi Wu and Changxi Zheng. 2022. Learning to Generate 3D Shapes from a Single Example. *ACM Transactions on Graphics (SIGGRAPH Asia)* 41, 6 (2022).
- Shuang Wu, Youtian Lin, Feihu Zhang, Yifei Zeng, Jingxi Xu, Philip Torr, Xun Cao, and Yao Yao. 2024a. Direct3D: Scalable Image-to-3D Generation via 3D Latent Diffusion Transformer. In *Conference on Neural Information Processing Systems (NeurIPS)*. 121859–121881.
- Shuang Wu, Youtian Lin, Feihu Zhang, Yifei Zeng, Yikang Yang, Yajie Bao, Jiachen Qian, Siyu Zhu, Xun Cao, Philip Torr, et al. 2025b. Direct3D-S2: Gigascale 3D Generation Made Easy with Spatial Sparse Attention. In *Conference on Neural Information Processing Systems (NeurIPS)*.
- Jianfeng Xiang, Zelong Lv, Sicheng Xu, Yu Deng, Ruicheng Wang, Bowen Zhang, Dong Chen, Xin Tong, and Jiaolong Yang. 2025. Structured 3D Latents for Scalable and Versatile 3D Generation. In *IEEE Conference on Computer Vision and Pattern Recognition (CVPR)*. 1–10.
- Zhiyu Xie, Yuqing Zhang, Xiangjun Tang, Yiqian Wu, Dehan Chen, Gongsheng Li, and Xiaogang Jin. 2024. StyleTex: Style Image-Guided Texture Generation for 3D Models. *ACM Transactions on Graphics (SIGGRAPH Asia)* 43, 6 (2024), 1–14.
- Kai Xu, Honghua Li, Hao Zhang, Daniel Cohen-Or, Yueshan Xiong, and Zhi-Quan Cheng. 2010. Style-Content Separation by Anisotropic Part Scales. In *ACM SIGGRAPH Asia 2010 papers*. 1–10.
- Kai Xu, Hao Zhang, Daniel Cohen-Or, and Baoquan Chen. 2012. Fit and Diverse: Set Evolution for Inspiring 3D Shape Galleries. *ACM Transactions on Graphics* 31, 4 (2012), 1–10.
- Hu Ye, Jun Zhang, Sibo Liu, Xiao Han, and Wei Yang. 2023. IP-Adapter: Text Compatible Image Prompt Adapter for Text-to-Image Diffusion Models. *arXiv preprint arXiv:2308.06721* (2023).
- Kangxue Yin, Jun Gao, Maria Shugrina, Sameh Khams, and Sanja Fidler. 2021. 3DStyleNet: Creating 3D Shapes with Geometric and Texture Style Variations. In *IEEE International Conference on Computer Vision (ICCV)*. 12456–12465.
- Xianfang Zeng, Xin Chen, Zhongqi Qi, Wen Liu, Zibo Zhao, Zhibin Wang, Bin Fu, Yong Liu, and Gang Yu. 2024. Paint3D: Paint Anything 3D with Lighting-Less Texture Diffusion Models. In *IEEE Conference on Computer Vision and Pattern Recognition (CVPR)*. 4252–4262.
- Xiaohui Zeng, Arash Vahdat, Francis Williams, Zan Gojcic, Or Litany, Sanja Fidler, and Karsten Kreis. 2022. LION: Latent Point Diffusion Models for 3D Shape Generation. In *Conference on Neural Information Processing Systems (NeurIPS)*.
- Biao Zhang, Jiapeng Tang, Matthias Nießner, and Peter Wonka. 2023b. 3DShape2VecSet: A 3D Shape Representation for Neural Fields and Generative Diffusion Models. *ACM Transactions on Graphics (SIGGRAPH)* 42, 4 (2023), 1–16 pages.
- Dingxi Zhang, Yu-Jie Yuan, Zhuoxun Chen, Fang-Lue Zhang, Zhenliang He, Shiguang Shan, and Lin Gao. 2025. StylizedGS: Controllable Stylization for 3D Gaussian Splatting. *IEEE Transactions on Pattern Analysis and Machine Intelligence* (2025).
- Longwen Zhang, Ziyu Wang, Qixuan Zhang, Qiewi Qiu, Anqi Pang, Haoran Jiang, Wei Yang, Lan Xu, and Jingyi Yu. 2024. CLAY: A Controllable Large-scale Generative Model for Creating High-quality 3D Assets. *ACM Transactions on Graphics (SIGGRAPH)* 43, 4 (2024), 1–20.
- Yuechen Zhang, Zexin He, Jinbo Xing, Xufeng Yao, and Jiaya Jia. 2023a. Ref-npr: Reference-based Non-photorealistic Radiance Fields for Controllable Scene Stylization. In *IEEE Conference on Computer Vision and Pattern Recognition (CVPR)*. 4242–4251.
- Zibo Zhao, Zeqiang Lai, Qingxiang Lin, Yunfei Zhao, Haolin Liu, Shuhui Yang, Yifei Feng, Mingxin Yang, Sheng Zhang, Xianghui Yang, et al. 2025. Hunyuan3D 2.0: Scaling Diffusion Models for High Resolution Textured 3D Assets Generation. *arXiv preprint arXiv:2501.12202* (2025).
- Howard Zhou, Jie Sun, Greg Turk, and James M Rehg. 2007. Terrain Synthesis from Digital Elevation Models. *IEEE Transactions Visualization & Computer Graphics* 13, 4 (2007), 834–848.



Fig. 8. Visual comparisons of geometry concept with Qwen-Edit [Wu et al. 2025a], Edit360 [Huang et al. 2025], StyleSculptor [Qu et al. 2025], Coin3D [Dong et al. 2024], and VoxHammer [Li et al. 2026]. Our results better preserve geometric attributes of the reference while more faithfully following text controls.



Fig. 9. Visual comparisons of appearance concept with Paint3D [Zeng et al. 2024], StyleTex [Xie et al. 2024], StyleSculptor [Qu et al. 2025]. Our method preserves the appearance attributes of the reference, while other approaches struggle with it.

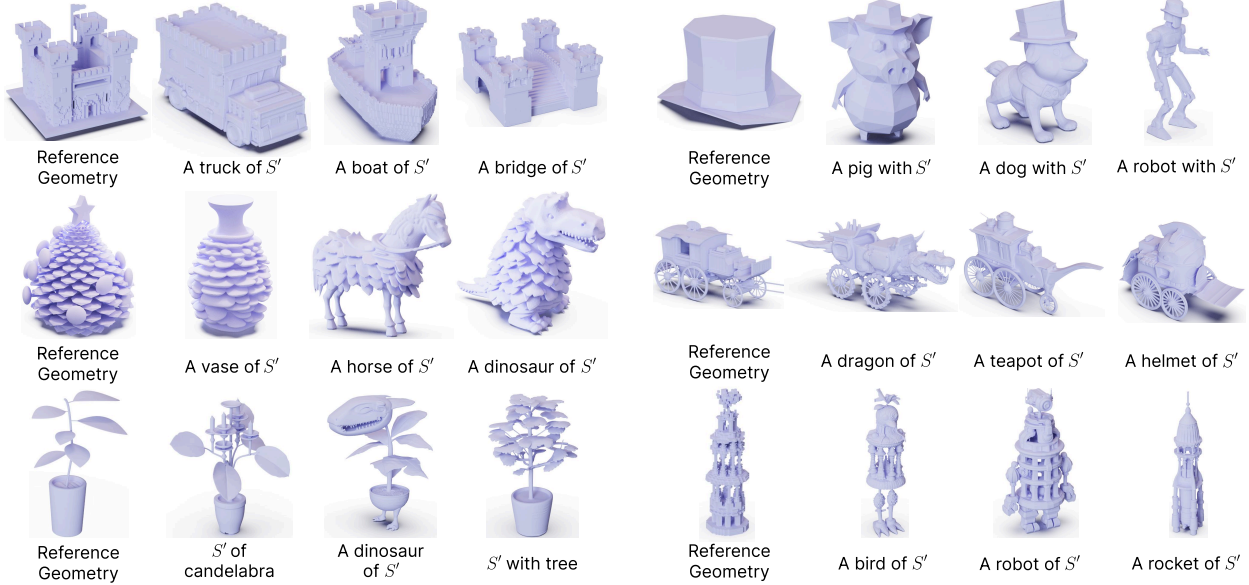


Fig. 10. Visual results for global geometry concept. Our method learns a global geometry concept from a reference shape and composes it with different text prompts to synthesize diverse shapes that consistently preserve the reference geometric attributes.

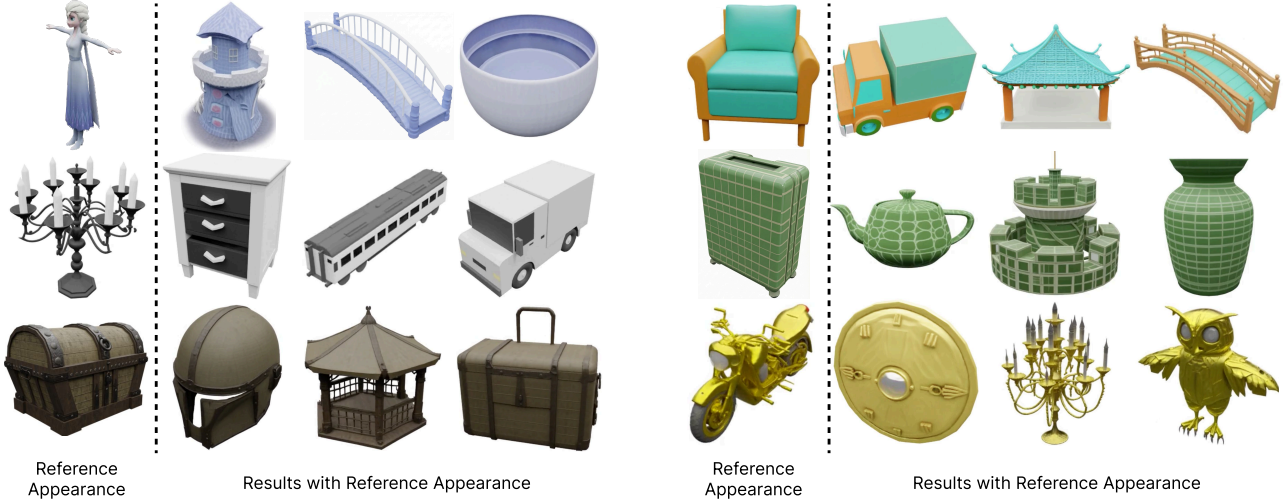


Fig. 11. Visual results for global appearance concept. By extracting global appearance concept, our approach produces multiple high-fidelity results that consistently reflect the reference appearance attributes.

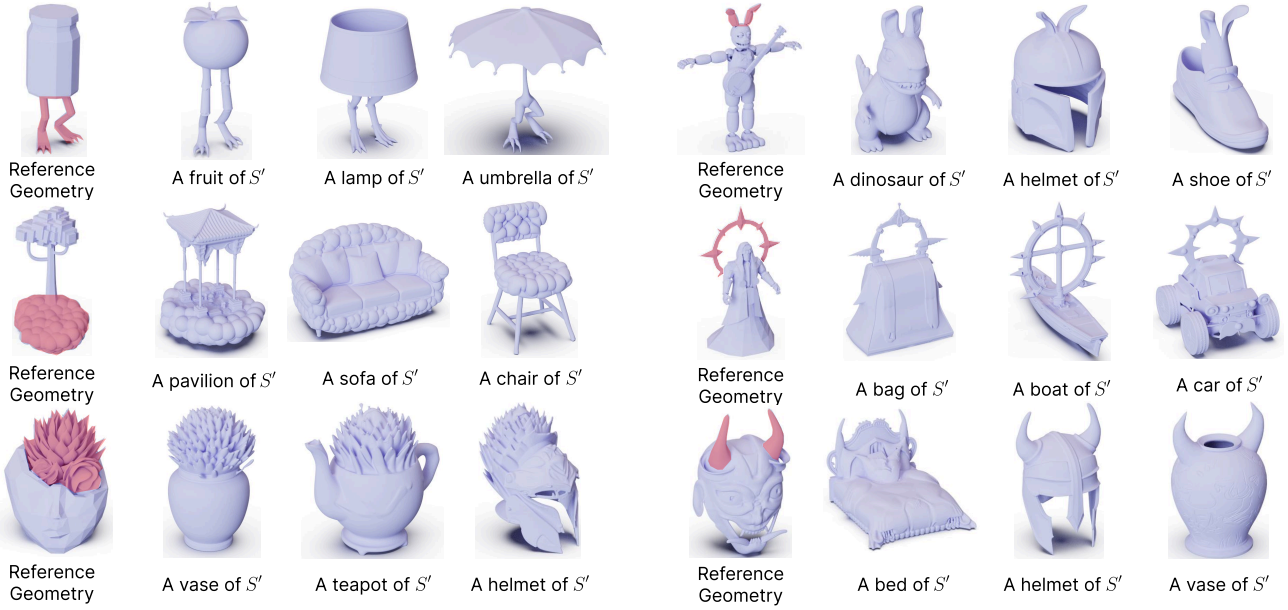


Fig. 12. Visual results for region-wise geometry concept. Our method enables extract the geometry concept from a user-specified region (marked in red), and compose it with text to generate novel shapes.

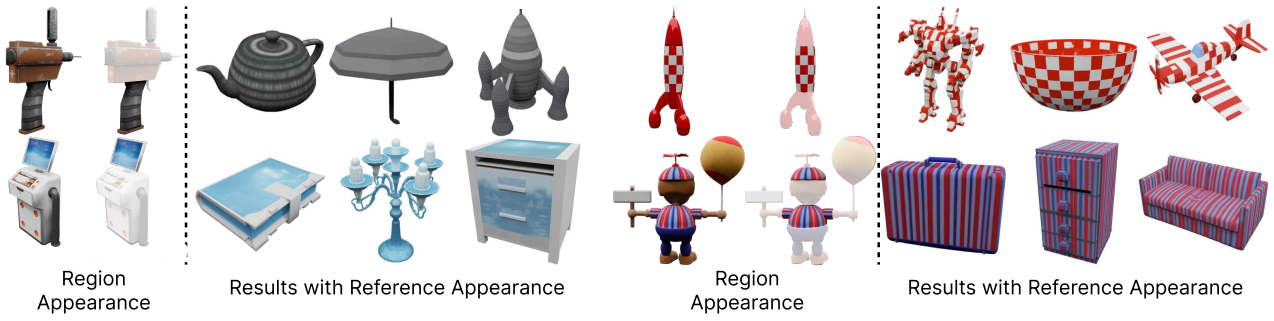


Fig. 13. Visual results for region-wise appearance concept. Our method enables extracting appearance concept from a localized region and reuse it to generate results that consistently inherit the reference appearance.